Evaluation of adsorption behavior for U(VI) and Nd(III) ions onto fumarated polystyrene microspheres

Ahmed R. Elsalamouny, Osman A. Desouky, Saad A. Mohamed, Ahmed A. Galhoum, Eric Guibal

▶ **To cite this version:**

Ahmed R. Elsalamouny, Osman A. Desouky, Saad A. Mohamed, Ahmed A. Galhoum, Eric Guibal. Evaluation of adsorption behavior for U(VI) and Nd(III) ions onto fumarated polystyrene microspheres. Journal of Radioanalytical and Nuclear Chemistry, 2017, 314 (1), pp.429-437. 10.1007/s10967-017-5389-5 . hal-02892696

HAL Id: hal-02892696
https://hal.science/hal-02892696

Submitted on 26 Jun 2024

HAL is a multi-disciplinary open access archive for the deposit and dissemination of scientific research documents, whether they are published or not. The documents may come from teaching and research institutions in France or abroad, or from public or private research centers.

L'archive ouverte pluridisciplinaire **HAL**, est destinée au dépôt et à la diffusion de documents scientifiques de niveau recherche, publiés ou non, émanant des établissements d'enseignement et de recherche français ou étrangers, des laboratoires publics ou privés.

Evaluation of adsorption behavior for U(VI) and Nd(III) ions onto fumarated polystyrene microspheres

Ahmed R. Elsalamouny[1] · Osman A. Desouky[1] · Saad A. Mohamed[2] · Ahmed A. Galhoum[1] · Eric Guibal[3]

Abstract Fumarated polystyrene microspheres were prepared using emulsion polymerization technique. Different instrumental techniques such as elemental analysis, SEM and FTIR were employed for full characterization of the synthetic resin. Different parameters such as pH, time and initial metal ions concentration were examined to evaluate the optimum conditions for U(VI) and Nd(III) ions sorption. For both metal ions, the sorption process fitted well with pseudo-second order kinetic model and Langmuir isotherm model. The maximum adsorption capacities were found to be 83.11 mg U g^{-1} and 39.68 mg Nd g^{-1}. The loaded sorbent was regenerated using 0.5 M HNO_3.

Keywords Neodymium · Sorption · Polystyrene · Microspheres · Fumaric acid

Introduction

Uranium is very essential element because of its strategic importance in the energy field [1]. Also, it is considered as a long-term potential environmental hazard as a result of its long half-life [2–4]. It is found in the environment in the hexavalent form, and it has biologically dynamic activity and chemical toxicity, leading to potential long-term harm to mammalian reproduction systems in the form of reduced fertility [5]. In addition, the uptake of uranium by human beings can cause irreparable damage, such as severe liver damage, kidney damage and eventually death [6]. Because of its high radiological and biological toxicity, it is necessary reducing its discharge into the environment due to activities of nuclear industry [7–10].

Rare earth elements (REEs) are widely used in High-technology and nuclear power industries [11–13]. The trivalent state is the most thermodynamically stable form of these elements in aqueous solutions [14]. Their physical and chemical properties are very close because of their close electronic configurations. The slight differences among lanthanide elements are so weak where the separation requires numerous steps [15]. Nd(III) was selected as a representative of trivalent lanthanide family. Because an ever-increasing demand for REEs in the international markets and limited resources for their production, the recovery of these metals from non-conventional resources is a strategic target.

Many conventional metal ions removal processes such as precipitation or solvent extraction processes face economical or technical limitations for the treatment of metal ions solutions. Adsorption process using mineral, ion-exchange or chelating resins may be more appropriate [16–22]. The chelating organic material can be copolymerized with an inert polymeric support like polystyrene and employed for the recovery of metal ions from aqueous solutions [23–26].

In the present work, a new chelating polymeric material (fumarated polystyrene resin) was prepared for enhanced sorption of uranyl and neodymium ions from aqueous solution. Fumaric acid was copolymerized with styrene monomers using emulsion polymerization technique.

✉ Ahmed R. Elsalamouny
hmd_sala@yahoo.com

[1] Nuclear Materials Authority, El-Maadi, P.O. Box 530, Cairo, Egypt

[2] Chemistry Department, Faculty of Science, Ain Shams University, Cairo, Egypt

[3] Ecole des mines d'Alès, Centre des Matériaux des Mines d'Alès (C2MA), 6 avenue de Clavières, 30319 Alès Cedex, France

Elemental analysis, scanning electron microscope (SEM) and FTIR were used to fully characterize the modified particles. Kinetic and isotherm studies were investigated to understand the adsorption behavior of metal ions on the synthetic resin.

Experimental

Preparation of fumarated polystyrene microspheres

Fumarated polystyrene microspheres were prepared using emulsion polymerization technique. 250 mL three necked round flask fitted with condenser, water bath and hot plate magnetic stirrer (Schott, Germany) was used. 7.8 mmol of fumaric acid (Sigma) was dissolved in a mixture of 3 mL styrene (Aldrich) and 0.9 mL divinylbenzene (Sigma-Aldrich). The solution was charged in the flask and 75 mL deionized water contains 0.37 mmol potassium persulfate and 0.5 mL Triton X-100 were added. After stirring of the mixture at 950 rpm for about 30 min, the stirring was continued for an additional 6 h at 75 °C. Finally, the cross-linked polymeric microspheres were collected and rinsed with ammonia solution and deionized water and dried for subsequent extraction studies.

Sorbent characterization

Thermo Finnigan Elemental Analytical Instrument (Italy) was used to determine the chemical composition of resin represented by the percentages of C, H, N and S. FTIR spectra were carried out using a PerkinElmer BX series with a frequency range of 4000–400 cm^{-1}. SEM/EDX analysis was performed on an environmental SEM (FEI Quanta 200 FEG) equipped with X-ray microanalyzer (OXFORD INCA ENERGY 350) to visualize surface morphology of sorbent and detect the elements and their semi-quantitative analysis.

Procedures

Adsorption behavior of metal ions on the sorbent was studied using batch experiments under different parameters. The resultant data is necessary for understanding the mechanisms of sorption and plays a fundamental role in assessing the suitability of sorbent for metal ions removal processes.

$UO_2(NO_3)_2{\cdot}6H_2O$ and $Nd(NO_3)_3{\cdot}6H_2O$ were used for the preparation of stock solutions (1000 mg L^{-1}). The working solutions were prepared by appropriate dilution of the stock solutions immediately prior to use.

Batch experiments were performed by contact of 0.02 g sorbent with 25 mL of 55 mg L^{-1} U(VI) or 57 mg L^{-1} Nd(III) ions solution in a polypropylene centrifuge tube at 20 °C and agitation 150 rpm. The solution pH was adjusted with NaOH or HNO_3 (0.1 M).

After equilibration and aqueous phase separation, the residual metal ions concentration in the aqueous phase was estimated by ICP-AES, while the concentration of adsorbed metal ions on the synthetic resin was estimated using the mass balance equation:

$$q = \frac{(C_i - C_e)V}{m} \quad (1)$$

where q (mg g^{-1}) is the amount of the adsorbed metal ions on the sorbent; C_i (mg L^{-1}) and C_e (mg L^{-1}) are the initial metal ion concentration and the residual metal ion concentration in the aqueous phase, respectively, V (L) is the volume of metal ions solution and m (g) is the weight of sorbent dosage.

Results and discussion

Characterization of sorbent

The experimental CHNS analysis data (%) of fumarated polystyrene microspheres are: C, 79.06; H, 7.5; N, 4.09; O, 9.35. The presence of nitrogen and oxygen shows the efficient chemical modification of polystyrene resin after copolymerization of fumaric acid with styrene monomers. Therefore, the resin formula is suggested to be $C_{22.6}H_{25.68}NO_{2.1}$.

For evaluation of the chemical modification, the FTIR spectra of the synthesized fumarated polystyrene resin was performed and compared with that of polystyrene resin (Fig. 1). Usually, the active functional groups are expected to exhibit characteristic peaks. The appearance of new bands at 1725 and 3205 cm^{-1}, assigned to C=O and N–H stretching vibrations, respectively.

Figure 2 illustrates SEM micrograph of fumarated polystyrene microspheres. The particles have a spherical morphology with a smooth surface and different sizes. The adsorbent also showed a mono-disperse structure.

Adsorption study

Effect of sorbent amount

The sorption of metal ions was studied by varying the amount of sorbent between 0.005 and 0.03 g 25 mL^{-1}. As shown in Fig. 3, the metal ions removal percentage increased as the sorbent amount increased and attained its maximum at 0.02 g. The removal efficiency becomes less significant after 0.02 g, leading to the decrease of sorption capacities of sorbent for metal ions. Thus, 0.02 g sorbent

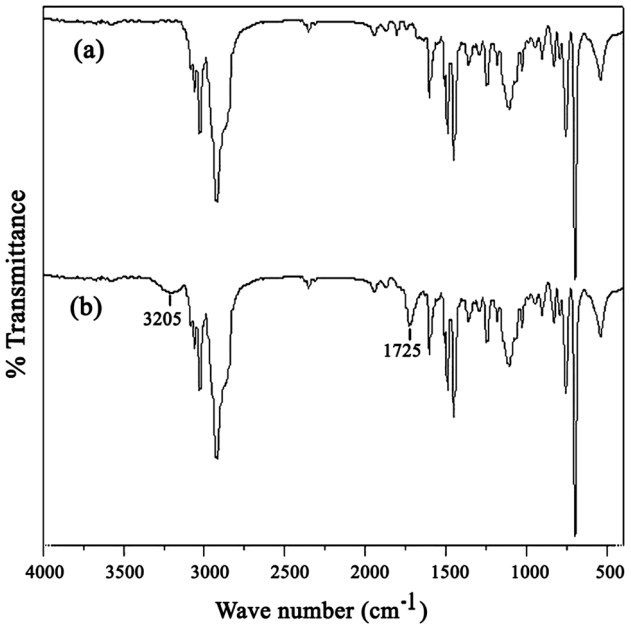

Fig. 1 FTIR spectra of (*a*) polystyrene and (*b*) fumarated polystyrene resin

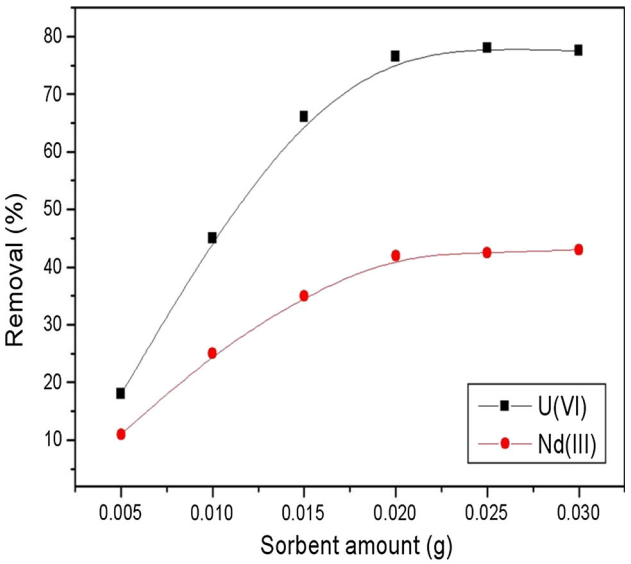

Fig. 3 Effect of sorbent amount on the uptake of U(VI) at pH 4 and Nd(III) at pH 5 where $V = 25$ mL and $C_i = 55$ mg U L^{-1} and 57 mg Nd L^{-1} at 20 °C

Fig. 2 SEM photo of fumarated polystyrene microspheres

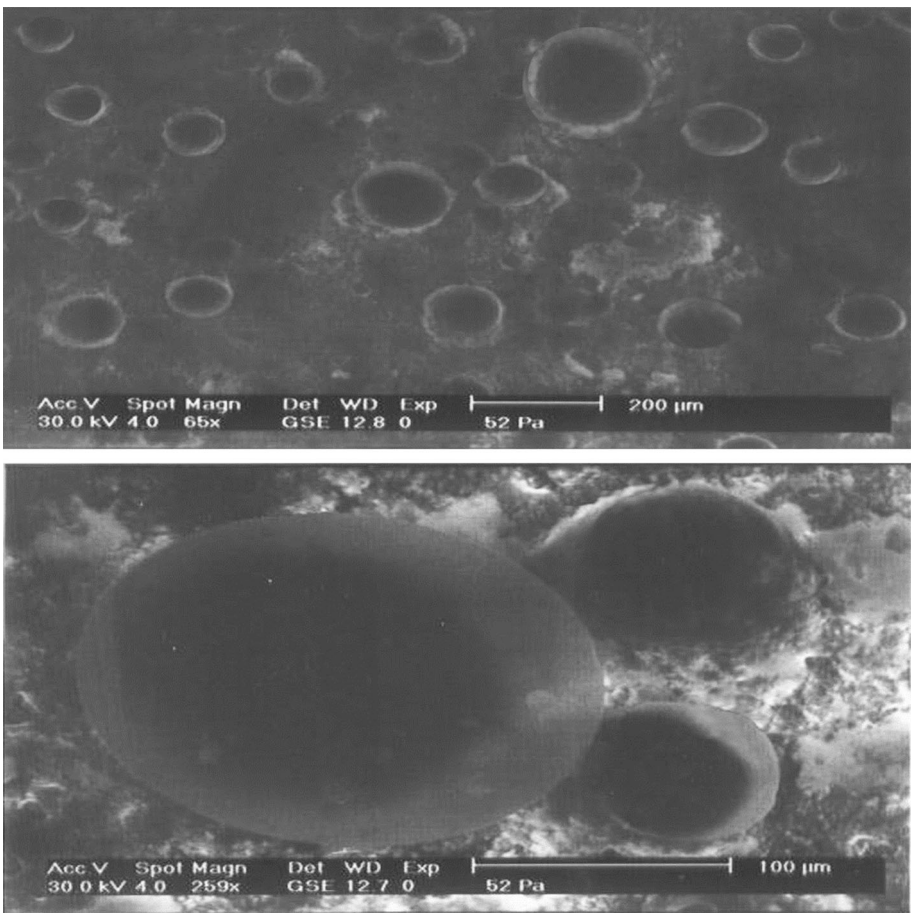

was chosen as the optimum sorbent amount for further experiments.

Effect of pH

The pH of the metal ions solution may affect the charge of sorbent surface or the dissociation degree of functional groups such as hydroxyl, carboxyl and amino groups present on the sorbent surface [27]. It can also affect the aqueous chemistry of metal ions and their competition for binding with active sites on the sorbent surface.

The metal ions removal from aqueous solutions was studied under non-competitive conditions at different pH as shown in Fig. 4. The sorption capacities of the synthetic resin increase significantly with increasing the initial pH range from 1 to 4.5 and 6 for uranyl and neodymium ions, respectively. The carboxylate groups ($-COO^-$) are responsible for the high efficiently enrichment of metal ions on the resin surface. According to the previous work, the additional peaks (e.g. Nd 3d, U 4f) are expected from XPS analysis of the loaded sorbent. Also, the relative intensity of O 1s decreases, indicating that oxygenated functional groups are responsible for the adsorption of U(VI) and Nd(III). Inner-sphere surface complexation is anticipated from EXAFS analysis for the adsorption of both metal ions onto microspheres resin [28–34].

The low adsorbed amounts for both metal ions at acidic media because the compensation of the negative charges on the sorbent by protons that suppress the sorption process [35, 36]. Also, the uptake for uranyl and neodymium ions decreases slightly at pH above 4.5 and 6, respectively, due to the hydrolysis of metal ions and other hydrolytic species are formed [31].

Kinetic study

Figure 5 shows the kinetic profiles of U(VI) and Nd(III) ions sorption on the sorbent in terms of adsorbed amount. Kinetic uptake was carried out under experimental conditions are comprised from optimum pH, an initial concentration of metal ions in the aqueous solution, 0.02 g of sorbent and agitation speed, 150 rpm at 20 °C. For U(VI) ions, The initial pH and concentration were set to 4 and 55 mg L^{-1}, respectively. While pH of 57 mg L^{-1} Nd(III) ions solution was adjusted to 5.

The kinetic removal for both metal ions was initially rapid due to the greater concentration gradient and more available sites for adsorption. A slower removal stage comes after and gradually approaches equilibrium. U(VI) ions reached equilibrium in 45 min, while the kinetic profile of Nd(III) ions was slower and the equilibrium time was 20 min. Over 92 and 90.5% of total adsorption of uranyl and neodymium ions occurred within the first 20 and 5 min, respectively.

Successive steps have been proposed in adsorption process such as bulk diffusion, film diffusion, intraparticle diffusion and adsorption uptake. The experimental data have been modeled using some conventional kinetic models to elucidate either the diffusion or adsorption is the rate limiting step.

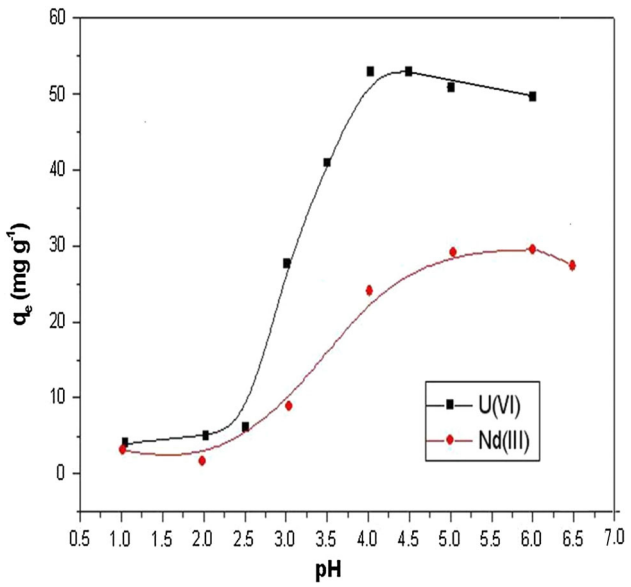

Fig. 4 Effect of pH on U(VI) and Nd(III) ions uptake using fumarated polystyrene resin where $V/m = 1.25$ L g^{-1} and $C_i =$ 55 mg U L^{-1} and 57 mg Nd L^{-1} at 20 °C

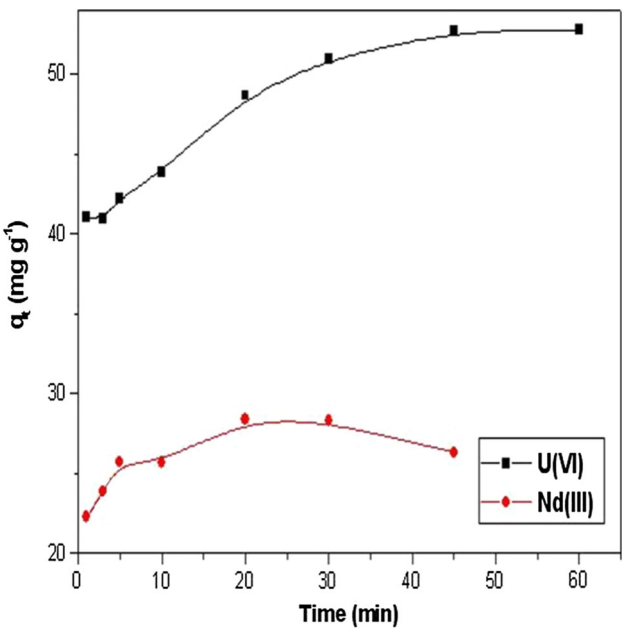

Fig. 5 Uptake kinetics of U(VI) at pH 4 and Nd(III) at pH 5 using fumarated polystyrene resin where $V/m = 1.25$ L g^{-1} and $C_i =$ 55 mg U L^{-1} and 57 mg Nd L^{-1} at 20 °C

Pseudo-first order rate equation (PFORE) [37]:

$$\log(q_e - q_t) = \log q_e - \frac{k_1}{2.303} t \quad (2)$$

where q_e and q_t (mg g^{-1}) are the retention capacities at equilibrium and time t, respectively, and k_1 is the Pseudo-first order rate constant (min^{-1}).

Pseudo-second order rate equation (PSORE) [38]:

$$\frac{t}{q_t} = \frac{1}{k_2 q_e^2} + \frac{1}{q_e} t \quad (3)$$

where k_2 is the Pseudo-second order rate constant (g mg^{-1} min^{-1}).

The chemical adsorption processes between metal ions and active sites were described using Elovich model as follow [39]:

$$q_t = \frac{1}{b} \ln(ab) + \frac{1}{b} \ln t \quad (4)$$

where b is constant related to the extent of surface coverage by metal ions and activation energy for chemisorption process (g mg^{-1}) and a is the initial adsorption rate (mg g^{-1} min^{-1}).

The analysis of diffusion mechanisms was performed using Crank equation. It can be used for roughly evaluating the intraparticle diffusion coefficient, D_e [40]:

$$\frac{q_e}{q_\infty} = 1 - \sum_{n=1}^{\infty} \frac{6\alpha(\alpha+1)}{9 + 9\alpha + q_n^2 \alpha^2} \exp \frac{-D_e q_n^2 t}{r^2} \quad (5a)$$

where r is the radius of the particle, while q_n and α are the non-zero roots and the ratio of the volumes of solution and particles from the following equations:

$$\tan q_n = \frac{3 q_n}{3 + \alpha q_n^2} \quad (5b)$$

$$\frac{q_\infty}{V C_i} = \frac{1}{1 + \infty}. \quad (5c)$$

The intraparticle diffusion coefficient value of neodymium ions (7.36×10^{-11} m^2 min^{-1}) is about one order of magnitude larger than uranyl ions (4.97×10^{-12} m^2 min^{-1}). Therefore, neodymium ions reach the equilibrium faster than uranyl ions. For both of uranyl and neodymium ions, the fitting processes have low correlation coefficients, 0.49 and 0.25, respectively, comparing with other kinetic models. Therefore, the diffusion of metal ions doesn't control the rate limiting step.

All constants of the sorption kinetic models are estimated including rate constants and equilibrium adsorbed amounts of metal ions on the sorbent surface and listed in Table 1. For both metal ions, the obtained correlation coefficient values (R^2) from the pseudo-second order model were higher than that of pseudo-first order model and Elovich equation. The calculated theoretical

Table 1 Kinetics parameters for U(VI) and Nd(III) ions sorption

Metal	q_{exp} (mg g^{-1})	PFORE			PSORE			Elovich equation	
		q_e (mg g^{-1})	k_1 (min^{-1})	R^2	q_e (mg g^{-1})	k_2 (g mg^{-1} min^{-1})	R^2	a (g g^{-1} min^{-1})	b (g mg^{-1})
U(VI)	52.8	14.54 ± 1.17	0.0666 ± 0.005	0.9777	53.5 ± 1.12	0.0148 ± 0.0037	0.9982	290 ± 20.41	0.2954 ± 0.044
Nd(III)	28.4	5.71 ± 1.52	0.0873 ± 0.041	0.6989	28.87 ± 0.82	0.0556 ± 0.0181	0.9975	180 ± 15.02	0.5177 ± 0.0705

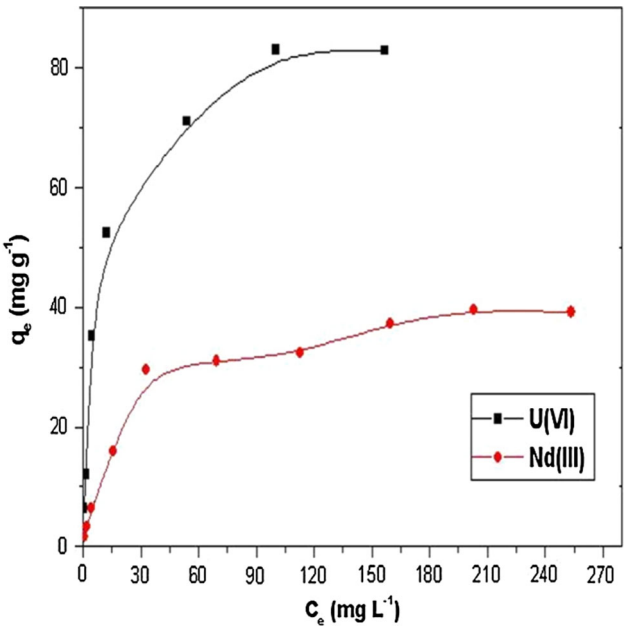

Fig. 6 Sorption isotherms of U(VI) at pH 4 and Nd(III) at pH 5 using fumarated polystyrene resin where $V/m = 1.25$ L g^{-1} at 20 °C

equilibrium adsorption capacities (53.5 ± 1.12 mg U g^{-1} and 28.87 ± 0.82 mg Nd g^{-1}) were very close to the actual (52.8 mg U g^{-1} and 28.4 mg Nd g^{-1}), indicating that the sorption for both metal ions onto the sorbent could be better explained by pseudo-second order model. Therefore, the rate limiting step is a chemical sorption involving valance forces through the sharing or exchange of electrons between the sorbent and adsorbates [6].

Sorption isotherm and thermodynamic study

Figure 6 shows the adsorbed amount of metal ions on the sorbent increases with increasing the residual metal ions concentration till the maximum capacity of the sorbent is reached. To obtain isotherm data for U(VI) or Nd(III) removal, batch experiments were performed by equilibrating 0.02 g of the sorbent and 25 mL of different initial metal ions concentrations at optimum pH and 20 °C.

The experimental data were tested using various isotherm models to determine the binding nature between metal ions and the sorbent surface [41]. The constants were evaluated and reported in Table 2.

Freundlich model:

$$\log q_e = \log K_F + \frac{\log C_e}{n} \quad (6)$$

where K_F and n are constants related to the adsorption capacity and the intensity of adsorption, respectively.

Table 2 Isotherm constants for U(VI) and Nd(III) ions sorption

Metal	q_{exp} (mg g^{-1})	Ferundlich equation			Langmuir equation			(D–R) equation		
		n	K_F	R^2	q_{max} (mg g^{-1})	K_L (L mg^{-1})	R^2	q_{max} (mg g^{-1})	E_{DR} (kJ mol^{-1})	R^2
U(VI)	83.11	2.14 ± 0.24	12.15 ± 2.23	0.9375	87.18 ± 2.93	0.1335 ± 0.0236	0.9953	378 ± 50.1	11.5 ± 0.52	0.964
Nd(III)	39.68	1.72 ± 0.14	2.38 ± 0.49	0.9485	43.1 ± 1.35	0.0407 ± 0.0046	0.9927	188.55 ± 18.02	9.65 ± 0.31	0.9744

Table 3 Comparison of sorption capacities of different sorbents for U(VI) and Nd(III) ions

Sorbent	Metal	Adsorption capacity (mg g^{-1})	References
p(GA–EGMA)–TAEA microbeads	U(VI)	64.3	[10]
Magnetite nanoparticles	U(VI)	5	[43]
Mannich type resin	U(VI)	5.084	[44]
Magnetic chitosan	U(VI)	42	[45]
Ethylenediamine-modified magnetic chitosan	U(VI)	82.83	[46]
Amberlite IRA-910 resin	U(VI)	11.9	[47]
This work	U(VI)	83.11	
Mordenite containing tuff	Nd(III)	13	[48]
Yeast cells	Nd(III)	10–12	[49]
Ion imprinted polymer particles	Nd(III)	33	[50]
This work	Nd(III)	39.68	

Langmuir model:

$$\frac{C_e}{q_e} = \frac{C_e}{q_{max}} + \frac{1}{K_L q_{max}} \tag{7}$$

where K_L is Langmuir adsorption constant (L mg^{-1}).

Dubinin–Radushkevich (D–R) model:

$$\ln q_e = \ln q_{max} - K_{DR}\varepsilon^2 \tag{8a}$$

ε (J mol^{-1}) is the Polanyi potential:

$$\varepsilon = RT\ln\left(1 + \frac{1}{C_e}\right) \tag{8b}$$

The mean-free sorption energy per molecule of adsorbate, E_{DR} (kJ mol^{-1}) is related to K_{DR} (mol^2 J^{-2}) and can be calculated from the following equation:

$$E_{DR} = \frac{1}{\sqrt{2K_{DR}}}. \tag{9}$$

E_{DR} gives information about the nature of sorption process of metal ions on the surface of sorbent (the discriminating value being physical < 8 kJ $mol^{-1} <$ chemical sorption) [42]. E_{DR} for uranyl and neodymium ions is 11.5 ± 0.52 and 9.65 ± 0.31 kJ mol^{-1}, respectively; this indicates that interaction between both metal ions and active sites comes through a chemisorption mechanism.

Sorption isotherm data are better simulated by Langmuir model compared to the other models with maximum sorption capacities (87.18 ± 2.93 mg U g^{-1} and 43.1 ± 1.35 mg Nd g^{-1}) and the highest correlation coefficients (0.9953 and 0.9927), respectively. This indicates that monolayer sorption was the main interaction mechanism of uranyl and neodymium ions with the sorbent.

The affinity of sorbent for binding of metal ions was evaluated using equilibrium parameter, R_L. The value of R_L was estimated from the following equation:

$$R_L = \frac{1}{1 + K_L C_i} \tag{10}$$

The R_L values are in the range of (0.58–0.04) and (0.92–0.09) for uranyl and neodymium ions, respectively. They lie between 0 and 1, indicating the affinity of sorbent for both metal ions removal. Table 3 shows that the experimental maximum capacities of the sorbent for both metal ions could be competitive when compared to some other previously prepared sorbents.

Thermodynamic behavior of the sorption processes for metal ions was evaluated using batch experiments under the same conditions in the range of temperatures from 20 to 50 °C. It was found that there is no significant variation in the sorption capacities of the new sorbent for both metal ions.

Sorbent selectivity

The uptake of metal ions was performed under non-competitive conditions to obtain the optimum parameters for removal processes. The sorbent selectivity was tested for both U(VI) and Nd(III) ions together in a binary solution at pH 4. The initial concentrations of U(VI) and Nd(III) ions were 0.47 and 0.64 mmol L^{-1}, respectively. After the equilibrium was reached, the residual concentration of Nd(III) ions about 0.54 mmol L^{-1} was higher than U(VI) ions, 0.358 mmol L^{-1}. This indicates that the sorbent has a high affinity toward U(VI) ions and the higher initial concentration of Nd(III) ions confirms it. It could be explained that the ionic radius of U(VI) is larger than Nd(III) where Nd(III) was affected by ionic radius contraction phenomenum. In addition, the 4f orbital of neodymium is effectively shielded from the strong interaction with ligand orbitals by electrons in the 5S and 5P orbitals [51].

Regeneration of sorbent

Metal ions removal from loaded sorbents is generally performed using diluted acidic solutions. The loaded sorbent (0.02 g) was desorbed using 25 mL of 0.5 M HNO_3 and shaking time of 1 h at 20 °C. The acid contaminants are washed with ammonia solution then distilled water after which it becomes ready for the next use. The results indicated that the sorption efficiency at the third run remains close to 96 and 94.5% of the initial value for uranium and neodymium ions sorption, respectively. Therefore, the reuse of resin remains appreciable.

Conclusion

Emulsion polymerization technique was employed for the synthesis of chelating microspheres based on fumaric acid modified polystyrene in presence of DVB as a cross-linker. Different instrumental techniques such as elemental analysis, FTIR, scanning electron microscope (SEM), were utilized for full characterization of the prepared polymeric resin.

For all studied systems, the kinetic and isotherm sorption data follow pseudo-second order rate equation and Langmuir equation, respectively. The maximum sorption capacities were 83.11 and 39.68 mg g^{-1} for U(VI) and Nd(III) ions, respectively. The temperature has no a significant effect on the variation in sorption capacities of the sorbent for both metal ions. Selectivity study indicates that fumarated polystyrene microspheres have high affinity to stabilize uranyl ions over Nd(III) ions in a binary solution.

References

1. Kumar A, Singhal RK, Rout S, Narayanan U, Karpe R, Ravi PM (2013) Adsorption and kinetic behavior of uranium and thorium in seawater-sediment system. J Radioanal Nucl Chem 295:649–656
2. Elsalamouny AR, Desouky OA, Mohamed SA, Galhoum AA, Guibal E (2017) Uranium and neodymium biosorption using novel chelating polysaccharide. Int J Biol Macromol 104:963–968
3. Zhang X, Ding C, Liu H, Liu L, Zhao C (2011) Protective effects of ion-imprinted Chitooligosaccharides as uranium-specific chelating agents against the cytotoxicity of depleted uranium in human kidney cells. Toxicology 286:75–84
4. Zou Y, Wang X, Wu F, Yu S, Hu Y, Song W, Liu Y, Wang H, Hayat T, Wang X (2017) Controllable synthesis of Ca–Mg–Al layered double hydroxides and calcined layered double oxides for the efficient removal of U(VI) from wastewater solutions. ACS Sustain Chem Eng. 5:1173–1185
5. Bayramoglu G, Arica MY (2016) MCM-41 silica particles grafted with polyacrylonitrile: modification into amidoxime and carboxyl groups for enhanced uranium removal from aqueous medium. Microporous Mesoporous Mater 226:117–124
6. Arica MY, Bayramoglu G (2016) Polyaniline coated magnetic carboxymethylcellulose beads for selective removal of uranium ions from aqueous solution. J Radioanal Nucl Chem 310:711–724
7. Meinrath G (1998) Aquatic chemistry of uranium. Geoscience 1:1–101
8. Rao TP, Metilda P, Gladis JM (2006) Preconcentration techniques for uranium(VI) and thorium(IV) prior to analytical determination—an overview. Talanta 68:1047–1064
9. Zou Y, Liu Y, Wang X, Sheng G, Wang S, Ai Y, Ji Y, Liu Y, Hayat T, Wang X (2017) Glycerol-modified binary layered double hydroxide nanocomposites for uranium immobilization via EXAFS technique and DFT theoretical calculation. ACS Sustain Chem Eng 5:3583–3595
10. Bayramoglu G, Arica MY (2017) Polyethylenimine and tris(2-aminoethyl)amine modified p(GA–EGMA) microbeads for sorption of uranium ions: equilibrium, kinetic and thermodynamic studies. J Radioanal Nucl Chem 312:293–303
11. Galhoum AA, Mahfouz MG, Abdel-Rehem ST, Gomaa NA, Atia AA, Vincent T, Guibal E (2015) Diethylenetriamine-functionalized chitosan magnetic nanobased particles for the sorption of rare earth metal ions [Nd(III), Dy(III) and Yb(III)]. Cellulose 22:2589–2605
12. Xu T, Peng H (2009) Formation cause, composition analysis and comprehensive utilization of rare earth solid wastes. J Rare Earths 27:1096–1102
13. Zhou J, Duan W, Zhou X, Zhang C (2007) Application of annular centrifugal contactors in the extraction flowsheet for producing high purity yttrium. Hydrometallurgy 85:154–162
14. Diniz V, Volesky B (2005) Biosorption of La, Eu and Yb using sargassum biomass. Water Res 39:239–247
15. Martins TS, Isolani PC (2005) Rare earths: industrial and biological applications. Quim Nova 28:111–117
16. Donia AM, Atia AA, Daher AM, Desouky OA, Elshehy EA (2011) Synthesis of amine/thiol magnetic resin and study of its interaction with Zr(IV) and Hf(IV) ions in their aqueous solutions. J Dispers Sci Technol 32:634–641
17. Roosen J, Binnemans K (2014) Adsorption and chromatographic separation of rare earths with EDTA- and DTPA-functionalized chitosan biopolymers. J Mater Chem A 2:1530–1540
18. Wang H, Ma L, Cao K, Geng J, Liu J, Song Q, Yang X, Li S (2012) Selective solid phase extraction of uranium by salicylideneimine-functionalized hydrothermal carbon. J Hazard Mater 229:321–330
19. Zou Y, Wang X, Khan A, Wang P, Liu Y, Alsaedi A, Hayat T, Wang X (2016) Environmental remediation and application of nanoscale zero-valent iron and its composites for the removal of heavy metal ions: a review. Environ Sci Technol 50:7290–7304
20. Erkaya IA, Arica MY, Akbulut A, Bayramoglu G (2014) Biosorption of uranium(VI) by free and entrapped Chlamydomonas reinhardtii: kinetic, equilibrium and thermodynamic studies. J Radioanal Nucl Chem 299:1993–2003
21. Bayramoglu G, Akbulut A, Arica MY (2015) Study of polyethyleneimine and amidoxime functionalized hybrid biomass of Spirulina (Arthrospira) platensis for adsorption of uranium (VI) ion. Environ Sci Pollut Res 22:17998–18010
22. Bayramoglu G, Arica MY (2016) Amidoxime functionalized Trametes trogii pellets for removal of uranium (VI) from aqueous medium. J Radioanal Nucl Chem 307:373–384
23. Bhattarai S, Kim J, Yun Y, Lee Y (2016) Preparation of polyaniline-coated polystyrene nanoparticles for the sorption of silver ions. React Funct Polym 105:52–59
24. Davarpanaha M, Ahmadpoura A, Rohani-Bastamia T, Dabirb H (2015) Synthesis and application of diethanolamine-

functionalized polystyrene as a new sorbent for the removal of *p*-toluenesulfonic acid from aqueous solution. J Ind Eng Chem 30:281–288
25. Kadous A, Didi MA, Villemin D (2010) A new sorbent for uranium extraction: ethylenediamino tris(methylenephosphonic) acid grafted on polystyrene resin. J Radioanal Nucl Chem 284:431–438
26. Mahfouz MG, Killa HM, Sheta ME, Moustafa AH, Tolba AA (2014) Synthesis, characterization, and application of polystyrene adsorbents containing tri-n-butylphosphate for solid-phase extraction of uranium (VI) from aqueous nitrate solutions. J Radioanal Nucl Chem 301:739–749
27. Crini G, Peindy HN, Gimbert F, Robert C (2007) Removal of C.I. Basic Green 4 (Malachite Green) from aqueous solutions by adsorption using cyclodextrin-based adsorbent: kinetic and equilibrium studies. Sep Purif Technol 53:97–110
28. Song W, Wang X, Wang Q, Shao D, Wang X (2015) Plasma-induced grafting of polyacrylamide on graphene oxide nanosheets for simultaneous removal of radionuclides. Phys Chem Chem Phys 17:398–406
29. Cheng W, Ding C, Wu Q, Wang X, Sun Y, Shi W, Hayat T, Alsaedi A, Chaicf Z, Wang X (2017) Mutual effect of U(VI) and Sr(II) on grapheme oxides: evidence from EXAFS and theoretical calculations. Environ Sci 4:1124–1131
30. Sun Y, Yang S, Chen Y, Ding C, Cheng W, Wang X (2015) Adsorption and desorption of U(VI) on functionalized graphene oxides: a combined experimental and theoretical study. Environ Sci Technol 49:4255–4262
31. Sun Y, Wu Z, Wang X, Ding C, Cheng W, Yu S, Wang X (2016) Macroscopic and microscopic investigation of U(VI) and Eu(III) adsorption on bacterium-derived carbon nanofibers. Environ Sci Technol 50:4459–4467
32. Sun Y, Wang X, Ai Y, Yu Z, Huang W, Chen C, Hayat T, Alsaedi A, Wang X (2017) Interaction of sulfonated graphene oxide with U(VI) studied by spectroscopic analysis and theoretical calculations. Chem Eng J 310:292–299
33. Wang X, Fan Q, Yu S, Chen Z, Ai Y, Sun Y, Hobiny A, Alsaedi A, Wang X (2016) High sorption of U(VI) on graphene oxides studied by batch experimental and theoretical calculations. Chem Eng J 287:448–455
34. Yin L, Wang P, Wen T, Yu S, Wang X, Hayat T, Alsaedi A, Wang X (2017) Synthesis of layered titanate nanowires at low temperature and their application in efficient removal of U(VI). Environ Pollut 226:125–134
35. Drits VA, Silvester E, Gorshkov AI, Manceau A (1997) Structure of synthetic monoclinic Na-rich birnessite and hexagonal birnessite: I. Results from X-ray diffraction and selected-area electron diffraction. Am Mineral 82:946–961
36. Peacock CL, Sherman DM (2007) Sorption of Ni by birnessite: equilibrium controls on Ni in seawater. Chem Geol 238:94–106
37. Lagergren S (1898) About the theory of so-called adsorption of soluble substances. Vetenskapsakademiens Handlingar 24:1–39
38. Ho YS, McKay G (1999) Pseudo-second order model for sorption processes. Process Biochem 34:451–465
39. Elwakeel KZ, Abd El-Ghaffar MA, El-Kousy SM, El-Shorbagy HG (2012) Synthesis of new ammonium chitosan derivatives and their application for dye removal from aqueous media. Chem Eng J 203:458–468
40. Crank J (1975) The mathematics of diffusion, 2nd edn. Oxford University Press, London
41. Foo KY, Hameed BH (2010) Insights into the modeling of adsorption isotherm systems. Chem Eng J 156:2–10
42. Ahmed IM, Gamal R, Helal AA, Abo-Elenein SA, Helal AA (2016) Kinetic sorption study of cerium (IV) on magnetite nanoparticles. Part Sci Technol. doi:10.1080/02726351.2016.1192572
43. Das D, Sureshkumar MK, Koley S, Mithal N, Pillai CGS (2010) Sorption of uranium on magnetite nanoparticles. J Radioanal Nucl Chem 285:447–454
44. Elsalamouny AR, Desouky OA, Mohamed SA, Galhoum AA (2017) Evaluation of adsorption behavior for U(VI) and Th(IV) ions onto solidified Mannich type material. J Dispers Sci Technol 38:860–865
45. Stopa LCB, Yamaura M (2010) Uranium removal by chitosan impregnated with magnetite nanoparticles: adsorption and desorption. Int J Nucl Energy Sci Technol 5:283–289
46. Wang JS, Peng RT, Yang JH, Liu YC, Hu XJ (2011) Preparation of ethylenediamine-modified magnetic chitosan complex for adsorption of uranyl ions. Carbohydr Polym 84:1169–1175
47. Rahmati A, Ghaemi A, Samadfam M (2012) Kinetic and thermodynamic studies of uranium(VI) adsorption using Amberlite IRA-910 resin. Ann Nucl Energy 39:42–48
48. Kozhevnikova NM, Tsybikova NL (2008) Sorption of neodymium(III) ions by natural mordenite-containing tuff. Russ J Appl Chem 81:42–45
49. Vlachou A, Symeopoulos BD, Koutinas AA (2009) A comparative study of neodymium sorption by yeast cells. Radiochim Acta 97:437–441
50. Krishna PG, Gladis JM, Rao TP, Naidu GR (2005) Selective recognition of neodymium(III) using ion imprinted polymer particles. J Mol Recognit 18:109–116
51. Tak RK, Gupta BD, Sobhash PD, Sharma A, Mathur SP (1990) Some rare earth chelates on N-thioacetyl-N-phenylhydroxylamine. Asian J Chem 2:132–135